*Am J Physiol Cell Physiol* 289: C564–C575, 2005.
First published April 20, 2005; doi:10.1152/ajpcell.00561.2004.

# $K^+$ channel $K_V$LQT1 located in the basolateral membrane of distal colonic epithelium is not essential for activating $Cl^-$ secretion

**Tianjiang Liao,[1] Ling Wang,[2] Susan Troutman Halm,[1] Luo Lu,[2] Robert E. W. Fyffe,[1] and Dan R. Halm[1]**

[1]*Department of Neuroscience, Cell Biology and Physiology, Wright State University, Dayton, Ohio; and* [2]*Division of Molecular Medicine, Harbor-UCLA Medical Center, David Geffen School of Medicine, University of California, Los Angeles, Torrance, California*

Submitted 19 November 2004; accepted in final form 12 April 2005

**Liao, Tianjiang, Ling Wang, Susan Troutman Halm, Luo Lu, Robert E. W. Fyffe, and Dan R. Halm.** $K^+$ channel $K_V$LQT1 located in the basolateral membrane of distal colonic epithelium is not essential for activating $Cl^-$ secretion. *Am J Physiol Cell Physiol* 289: C564–C575, 2005. First published April 20, 2005; doi:10.1152/ajpcell.00561.2004.—The cellular mechanism for $Cl^-$ and $K^+$ secretion in the colonic epithelium requires $K^+$ channels in the basolateral and apical membranes. Colonic mucosa from guinea pig and rat were fixed, sectioned, and then probed with antibodies to the $K^+$ channel proteins $K_V$LQT1 (*Kcnq1*) and minK-related peptide 2 (MiRP2, *Kcne3*). Immunofluorescence labeling for *Kcnq1* was most prominent in the lateral membrane of crypt cells in rat colon. The guinea pig distal colon had distinct lateral membrane immunoreactivity for *Kcnq1* in crypt and surface cells. In addition, *Kcne3*, an auxiliary subunit for *Kcnq1*, was detected in the lateral membrane of crypt and surface cells in guinea pig distal colon. Transepithelial short-circuit current ($I_{sc}$) and transepithelial conductance ($G_t$) were measured for colonic mucosa during secretory activation by epinephrine (EPI), prostaglandin $E_2$ ($PGE_2$), and carbachol (CCh). HMR1556 (10 μM), an inhibitor of *Kcnq1* channels (Gerlach U, Brendel J, Lang HJ, Paulus EF, Weidmann K, Brüggemann A, Busch A, Suessbrich H, Bleich M, and Greger R. *J Med Chem* 44: 3831–3837, 2001), partially (~50%) inhibited $Cl^-$ secretory $I_{sc}$ and $G_t$ activated by $PGE_2$ and CCh in rat colon with an $IC_{50}$ of 55 nM, but in guinea pig distal colon $Cl^-$ secretory $I_{sc}$ and $G_t$ were unaltered. EPI-activated $K^+$-secretory $I_{sc}$ and $G_t$ also were essentially unaltered by HMR1556 in both rat and guinea pig colon. Although immunofluorescence labeling with a *Kcnq1* antibody supported the basolateral membrane presence in colonic epithelium of the guinea pig as well as the rat, the *Kcnq1* $K^+$ channel is not an essential component for producing $Cl^-$ secretion. Other $K^+$ channels present in the basolateral membrane presumably must also contribute directly to the $K^+$ conductance necessary for $K^+$ exit during activation of $Cl^-$ secretion in the colonic mucosa.

HMR1556; $K^+$ secretion; epinephrine; prostaglandin $E_2$; cholinergic

ABSORPTION AND SECRETION of ions across the colonic epithelium produces an osmotic driving force for fluid flow that modifies the volume and composition of the luminal fluid, and these ion transport processes have been examined extensively in the colon of rats and guinea pigs (11, 27, 50). The cellular mechanisms for active $Na^+$ absorption and $Cl^-$ secretion in particular depend on $Na^+/K^+$ pumps and $K^+$ channels in the basolateral membranes to produce appropriate electrochemical driving forces for ion flow across both the apical and basolateral membranes. Various secretagogues also stimulate electrogenic $K^+$ secretion, together with $Cl^-$ secretion (11, 30, 41, 53), which requires the presence of $K^+$ channels in apical membranes. Thus $K^+$ channels are central to the ion transport function of these epithelial cells. The identity of the $K^+$ channels involved in $Cl^-$ secretion has been examined by patch-clamp recording, particularly during manipulations of intracellular cAMP and $Ca^{2+}$. From these studies, voltage-sensitive $K^+$ channels ($K_V$)LQT1 (*Kcnq1*) have been proposed to support cAMP-dependent secretagogue activation, whereas IK1 (*Kcnn4*) $K^+$ channels would support $Ca^{2+}$-dependent activation (24, 63).

The colonic epithelium of mammals is composed of a relatively flat surface epithelium invaginated by numerous crypts of Lieberkühn (12). Within this epithelium, columnar cells and goblet cells are the predominant cell types, with a minor population of enteroendocrine cells. Goblet cells are distinguished from columnar cells by a large, dense cluster of apical mucous granules (59). Other cell types also are present in the colonic mucosa, including myoepithelial cells forming the pericryptal sheath, capillaries, and nerve fibers, as well as various types of leukocytes (8, 9, 48, 51). Previous studies support the concept that crypt columnar cells are major contributors to transepithelial ion secretion and mucus release (28, 29, 31, 32).

The two types of $K^+$ channels proposed as the major components of basolateral membrane $K^+$ conductance that support colonic $Cl^-$ secretion, *Kcnn4* and *Kcnq1*, have been observed in cells of isolated colonic crypts (24, 63). The intermediate conductance inwardly rectifying $K^+$ channel, *Kcnn4*, could be the $Ca^{2+}$-activated basolateral membrane $K^+$ conductance supporting cholinergic stimulation (34, 63). In addition, a $Ca^{2+}$-dependent inward rectifier that may be *Kcnn4* has been observed in human colonic crypts (56). Association of *Kcnq1* with minK-related peptide 2 (MiRP2, *Kcne3*) produces a cAMP-activated basolateral membrane $K^+$ conductance (24, 63) that could support $Cl^-$-secretory activation by secretagogues such as vasoactive intestinal peptide or prostaglandin $E_2$ ($PGE_2$) (11, 27, 50), and both of these channel proteins have been localized to lateral membranes of mouse colonic crypts (14, 58). The involvement of *Kcnq1/Kcne3* ($K_V$LQT1/MiRP2) $K^+$ channels in colonic $Cl^-$ secretion is supported further by the inhibition of cAMP-dependent secretion and channel activity by the chromanol 293B (24, 43, 58, 63). In contrast, even though 293B inhibited cAMP-dependent $K^+$ currents in pancreatic acinar cells consistent with *Kcnq1/Kcne1* (37, 62), 293B did not inhibit fluid secretion (38). However, the importance of cAMP as an intracellular signal that modulates secretory activity still makes the cellular location of *Kcnq1* a useful indicator of possible secretory function.

Address for reprint requests and other correspondence: D. R. Halm, Dept. of Neuroscience, Cell Biology and Physiology, Wright State Univ., 3640 Colonel Glenn Hwy., Dayton, OH 45435 (e-mail: dan.halm@wright.edu).

The costs of publication of this article were defrayed in part by the payment of page charges. The article must therefore be hereby marked "*advertisement*" in accordance with 18 U.S.C. Section 1734 solely to indicate this fact.

Secretagogues operating through cAMP-dependent mechanisms produce two distinct modes of electrogenic ion secretion in the colonic epithelium (27, 30, 41). The more familiar mode involves $Cl^-$ secretion that is also accompanied by electrogenic $K^+$ secretion. This flow of ions into the lumen creates fluid buildup in crypt lumens, producing fluid flow that sweeps along mucus and other material (28), such that the term flushing secretion best summarizes the action of these secretagogues. The second secretory mode produces electrogenic $K^+$ secretion, but without large, sustained $Cl^-$ secretion. Modulatory secretion is a useful term to conceptualize this secretory function because fluid flow is low, but ion composition would be altered. Rat and guinea pig distal colon both produce these modes of secretion (53, 64), with differences in rates that may serve the specific physiology of an omnivore and a herbivore, respectively (52, 54). Thus a comparison of these two modes of secretion in these species can be used to demonstrate the varied roles of basolateral membrane $K^+$ channels. In particular, increased basolateral membrane $K^+$ channel activity would aid $Cl^-$ secretion by enhancing the electrochemical driving force for conductive apical $Cl^-$ exit, whereas decreased activity could increase $K^+$ secretion by limiting basolateral exit of $K^+$ into the interstitial space (40). The focus of this study was to examine the epithelial location of *Kcnq1/Kcne3* $K^+$ channels in the colon and to use the chromanol derivative HMR1556 (22) to determine the involvement of this $K^+$ channel type in secretory activation by physiological secretagogues.

## METHODS

Guinea pigs (Hartley, male, 400- to 650-g body wt) and rats (Sprague-Dawley, male or female, 125- to 250-g body wt) were administered standard chow and water ad libitum. In accordance with protocols approved by the Wright State University Laboratory Animal Care and Use Committee, guinea pigs and rats were killed by decapitation or by administration of an intraperitoneal overdose (>80 mg/kg) of pentobarbital sodium before perfusion fixation. The colon was removed, cut open along the mesenteric line, and flushed with saline solution to remove fecal pellets. The mucosa was separated from underlying submucosa and external muscle layers using a glass slide to gently scrape along the length of the colonic sheet, thus producing an isolated mucosal preparation (3, 9, 15). Because the plane of dissection occurred at the base of the crypts, the muscularis mucosae also were removed. Tissue samples were taken from the distal colon of the guinea pig (54), at distances of 5–20 cm (late) and ~40 cm (early) from the peritoneal border. Colonic tissue samples from rat (~12 cm total length) were taken from the proximal portion that had palm leaf mucosal folds and from the distal 1–5 cm measured from the peritoneal border (17, 19, 42).

*Tissue fixation.* Colonic tissues were fixed either by perfusion of fixative or after isolation of the mucosa. For perfusion-fixation, animals were perfused transcardially (20) with a vascular rinse solution (4°C), followed by 4% paraformaldehyde in phosphate buffer (PB). The colon was removed, cut into annuli, and postfixed with 4% paraformaldehyde in PB for 1 h. Perfusion-fixation did not produce satisfactory structural preservation in guinea pig colonic mucosa. Fixation also was accomplished by pinning isolated mucosal sheets in a Sylgard-coated dish for immersion in fixation solutions. Each mucosal specimen was fixed in PB containing 1% paraformaldehyde and 0.125% glutaraldehyde (15 min at room temperature). The mucosal specimens were fixed further in PB with 4% paraformaldehyde (20 min at room temperature). Chemicals used for the preparation of solutions were obtained from Sigma Chemical (St. Louis, MO). Vascular rinse solution contained (in mM) 161 $Na^+$, 3.4 $K^+$, 140 $Cl^-$, 6.0 $HCO_3^-$, 1.9 $H_2PO_4^-$, and 8.1 $HPO_4^{2-}$. PB contained (in mM) 181 $Na^+$, 19 $H_2PO_4^-$, and 81 $HPO_4^{2-}$. Phosphate-buffered saline (PBS) contained (in mM) 168 $Na^+$, 2.7 $K^+$, 153 $Cl^-$, 1.9 $H_2PO_4^-$, and 8.1 $HPO_4^{2-}$. Tris-buffered saline (TBS) contained (in mM) 137 $Na^+$, 155 $Cl^-$, and 20 Tris.

*Immunolocalization.* Mucosal tissues were prepared for immunofluorescence (2, 20) by dehydration in PB (4°C) with sucrose (15% wt/vol) and then frozen with optimal cutting temperature compound. Sections were cut (6 μm) on a cryostat and thaw mounted on gelatin-coated slides. Sections were permeabilized with PBST (PBS with 0.1% Triton X-100; 30 min), blocked in PBST with normal horse serum (10%, 1 h, room temperature), and then incubated (4°C) overnight with primary antibody in PBST. The following antibodies for $K^+$ channel and auxiliary subunits were obtained from commercial suppliers (Chemicon International, Temecula, CA; Santa Cruz Biotechnology, Santa Cruz, CA; Jackson ImmunoResearch, West Grove PA): polyclonal anti-$K_V$LQT1 (6.5 ng/μl; Chemicon, COOH-terminal residues of human *Kcnq1*), two polyclonal anti-*Kcne3* [4.0 ng/μl, Santa Cruz Biotechnology, internal domain (L-20) and $NH_2$-terminal residues (N-18) of human *Kcne3*], and polyclonal anti-metabotropic glutamate receptor (1.0 ng/μl, Chemicon; residues 1180–1191 of rat mGluR1-α, *Grm1*). After being washed three times in PBS, sections were incubated in the dark with the appropriate secondary antibodies (Jackson ImmunoResearch) and donkey-anti-rabbit or donkey-anti-goat IgG antibody conjugated to fluorescein isothiocyanate (FITC; 15 ng/μl for 2 h at room temperature). Sections were washed and mounted in Vectashield (Vector Laboratories, Burlingame, CA). Absorption controls were preformed by preincubation of primary antibody with the antigenic peptide in PBS (60–90 min at room temperature) before addition to sections. Fluorescence was visualized using an Olympus BX60 epifluorescence microscope.

Detection of ion channel proteins also was accomplished using immunoblot analysis. Isolated colonic mucosa was disrupted by performing sonication in a buffered solution containing protease inhibitors (on ice). The isolation solution contained (in mM) 178 $Na^+$, 1.5 $Mg^{2+}$, 153 $Cl^-$, 50 HEPES, 10 EDTA, 10% glycerol, 1% Triton X-100, and 1.0 4-(2-aminoethyl)benzenesulfonyl fluoride, as well as (in μM) 1.54 aprotinin, 23.5 leupeptin, and 14.6 pepstatin A. Samples were centrifuged at 6,000 *g* (for 10 min at 4°C) followed by centrifugation of the resulting supernatant at 100,000 *g* (for 60 min at 4°C) to obtain a membrane sample; protein content was determined using the Bradford method (7). Proteins were electrophoresed by performing SDS-PAGE and transferred to polyvinylidene difluoride (PVDF) membranes. These membranes were blocked with 10% nonfat dry milk in TBST (TBS with 0.1% Tween 20), followed by incubation with specific primary antibody and then with horseradish peroxidase-conjugated secondary antibody. Membranes were developed (90 s) with LumiGLO (Cell Signaling Technology, Beverly, MA) before film was exposed to detect the product.

*Transepithelial current measurement.* Isolated mucosal sheets were used for measurement of transepithelial current and conductance (30, 53). Four mucosal sheets from each animal were mounted in Ussing chambers (0.64-$cm^2$ aperture) and supported on the serosal face by Nuclepore filters (~10 μm thick, 5-μm pore diameter; Whatman, Clifton NJ). Bathing solutions (10 ml) were circulated by gas lift through water-jacketed reservoirs (38°C). Standard Ringer solution contained (in mM) 145 $Na^+$, 5.0 $K^+$, 2.0 $Ca^{2+}$, 1.2 $Mg^{2+}$, 125 $Cl^-$, 25 $HCO_3^-$, 4.0 $H_{(3-X)}PO_4^{X-}$, and 10 D-glucose. Solutions were continually gassed with 95% $O_2$-5% $CO_2$, which maintained the solution at pH 7.4. Chambers were connected to automatic voltage clamps (Physiologic Instruments, San Diego, CA) that permitted compensation for solution resistance and continuous measurement of short-circuit current ($I_{sc}$). Transepithelial electrical potential difference was measured using paired calomel electrodes connected to the chambers by Ringer-agar bridges. Current was passed across the tissue through two Ag-AgCl electrodes connected by Ringer-agar bridges. $I_{sc}$ was referred to as positive for flow across the epithelium from the mucosal to the serosal side. Transepithelial conductance ($G_t$)

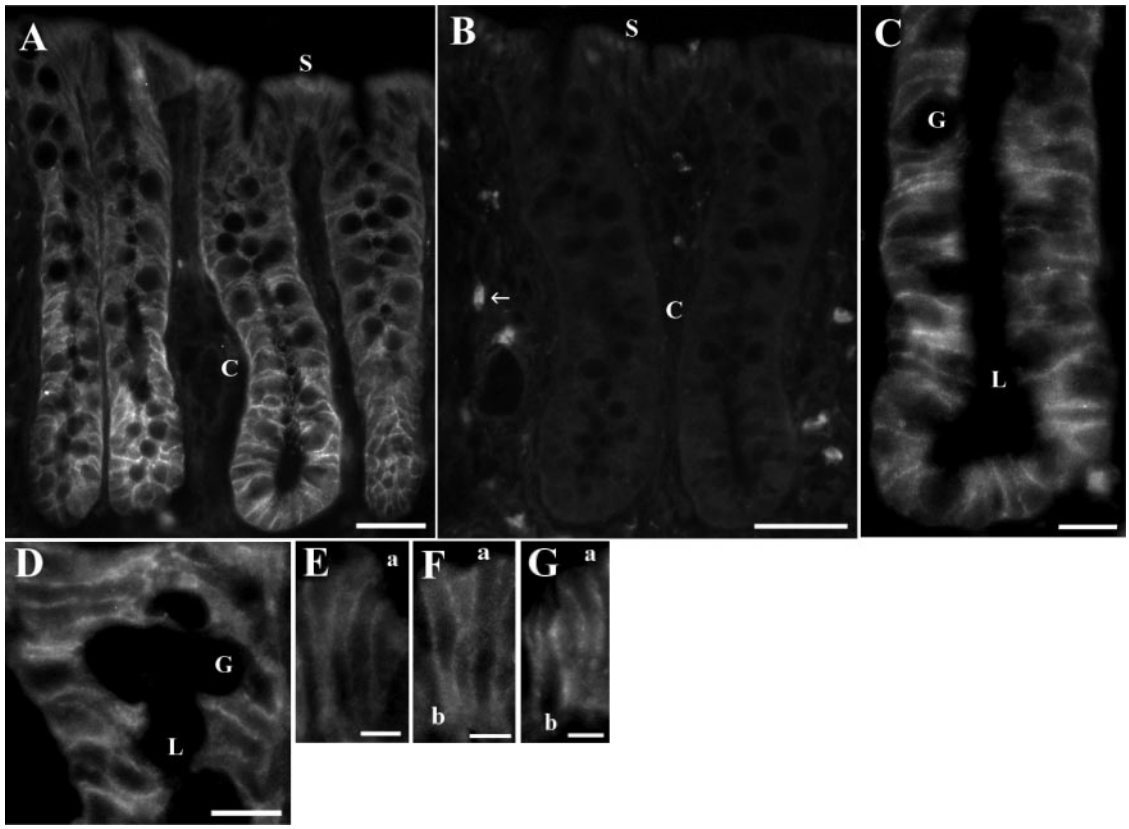


Fig. 1. Localization of $K^+$ channel $K_V$LQT1 (*Kcnq1*) immunoreactivity in rat colonic mucosa. *Kcnq1* was detected using immunofluorescence in rat colonic mucosa, fixed either by perfusion or after isolation (anti-$K_V$LQT1; Chemicon). *A*: crypt (C) and surface (S) epithelia are shown from a perfusion-fixed specimen of distal colon. Lateral membranes of crypt cells labeled distinctly. *B*: in perfusion-fixed distal colon with secondary antibody alone, nonspecific labeling and autofluorescence of epithelial cells was low, but mucosal leukocytes (arrow) showed nonspecific labeling. *C*: crypt from a perfusion-fixed distal colon specimen with a longitudinal profile of the lumen (L) showed a lack of apical membrane labeling, together with lateral membrane labeling. Some goblet cells (G) were apparent by the rounded cellular profiles with dark, round apical poles. Basal cell poles suggested labeling for only some cells. *D*: longitudinal profile of a crypt from a proximal colon specimen fixed as an isolated mucosa showed lateral membrane labeling and a lack of apical membrane labeling. Some goblet cells (G) were apparent by the dark round apical poles. Surface epithelium in proximal (*E*) and distal (*F* and *G*) colon specimens fixed as isolated mucosa showed faint but distinct labeling of lateral membranes without any indication of apical (a) or basal (b) membrane labeling. Scale bars, 25 μm for *A* and *B*; 10 μm for *C* and *D*; and 5 μm for *E–G*.

was calculated on the basis of currents produced by bipolar square voltage pulses imposed across the mucosa (±5 mV, 3-s duration, 1-min intervals).

$PGE_2$, indomethacin, and NS398 were obtained from Cayman Chemical (Ann Arbor, MI), and epinephrine (EPI) was purchased from Elkins-Sinn (Cherry Hill, NJ). $K^+$ channel blockers HMR1556 {(3R,4S)-(+)-*N*-[3-hydroxy-2,2-dimethyl-6-(4,4,4-trifluorobutoxy) chroman-4-yl]-*N*-methylethanesulfonamide} and 293B [*trans*-6-cyano-4-(*N*-ethylsulfonyl-*N*-methylamino)-3-hydroxy-2,2-dimethylchromane] were provided by Dr. Uwe Gerlach (Aventis Pharma Deutschland, Frankfurt-am-Main, Germany). All other chemicals were obtained from Sigma Chemical. Drugs were added in small volumes from concentrated stock solutions. $PGE_2$ was prepared in an ethanol stock solution that added 0.03% ethanol at 3 μM $PGE_2$. Stock solutions of HMR1556 (10 mM) and 293B (100 mM) were made with DMSO. Additions of 1% ethanol or DMSO alone did not alter transepithelial measures of $K^+$ or $Cl^-$ secretion (*30*).

Inhibitor-sensitive components of $I_{sc}$ and $G_t$ were calculated using the paired responses of adjacent mucosal tissues. Stripchart recordings of $I_{sc}$ were digitized at 10-s intervals to examine secretory onset. Concentration responses of $I_{sc}$ to inhibitors were fit to Henri-Michaelis-Menten binding curves using a nonlinear least-squares procedure (30). Results are reported as means ± SE. Statistical comparisons were performed using a two-tailed Student's *t*-test for paired responses, with statistically significant differences accepted at $P < 0.05$.

## RESULTS

*Localization of $K^+$ channel subunits Kcnq1 and Kcne3.* Immunoreactivity for the $K^+$ channel protein $K_V$LQT1, *Kcnq1*, was detected in a location consistent with the plasma membrane of colonic epithelial cells (Figs. 1 and 2) in accordance with previous reports in which immunolocalization (14, 62) and patch-clamp recording of channel activity were used (24, 58). Similar to mouse colon (14, 62), the rat colon (Fig. 1*A*) had prominent labeling in the lateral membrane of crypt epithelial cells, but surface epithelial cells did not exhibit clear labeling in the perfusion-fixed specimens. Rat mucosa fixed after isolation had lower background in surface epithelial cells than in perfusion-fixed specimens, such that faint but distinct labeling of lateral membranes was apparent in surface cells of rat proximal and distal colon (Fig. 1, *E–G*). The luminal margins of either crypt or surface epithelial cells were not labeled (Fig. 1), supporting an absence of *Kcnq1* from the apical membranes of these epithelial cells. Similar results were obtained for the proximal colon (Fig. 1, *D* and *E*) and distal colon (Fig. 1, *C*, *F*, and *G*).

Isolated mucosa of guinea pig distal colon also showed labeling for *Kcnq1* in the lateral membranes of both crypt and

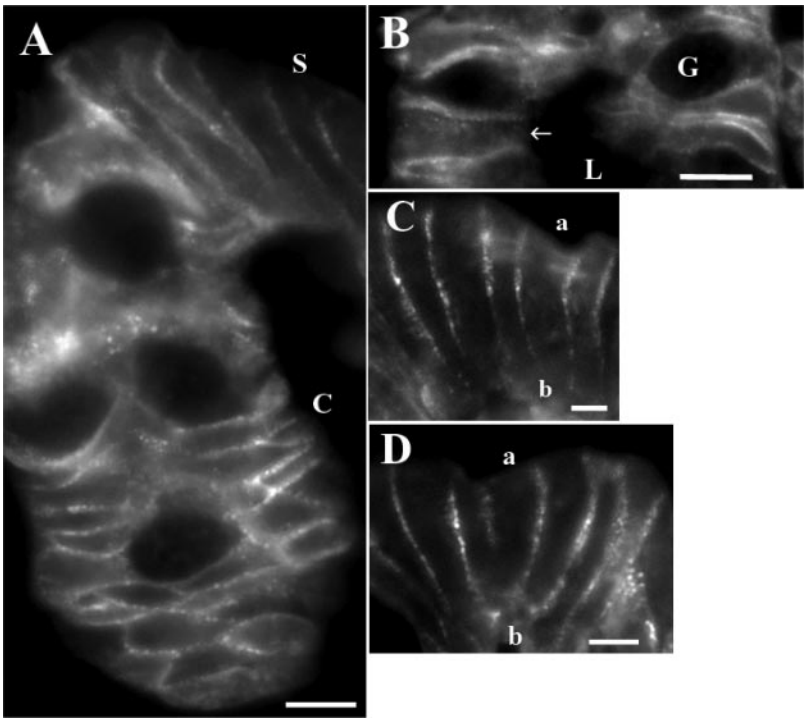


Fig. 2. Localization of *Kcnq1* immunoreactivity in guinea pig distal colonic mucosa. *Kcnq1* was detected using immunofluorescence in guinea pig distal colonic mucosa fixed after isolation (anti-$K_V$LQT1; Chemicon). *A*: lateral membranes of crypt and surface cells showed distinct labeling. When the secondary antibody alone was applied, nonspecific labeling of epithelial cells was low (data not shown). *B*: crypt with a longitudinal profile of the lumen (L) showed the lack of apical membrane labeling (arrow), together with lateral membrane labeling. Some goblet cells (G) were apparent because of the rounded cellular profiles with dark apical poles. Basal membrane labeling was not distinctly apparent for columnar cells. Epithelial profiles of surface epithelium (*C* and *D*) showed labeling extending along the length of the lateral margin of columnar cells without any labeling in the apical membrane (a) and only weak labeling if any indications of labeling were observed in the basal membrane (b) region. Scale bars, 10 μm for *A* and *B*; 5 μm for *C* and *D*.

surface epithelial cells (Fig. 2), with similar results for both early and late portions. This prominent lateral membrane labeling had a beaded appearance suggesting a clustering of sites. The apical membrane of both the crypt (Fig. 2*B*) and the surface epithelium (Figs. 2, *C* and *D*) from guinea pig distal colon lacked any detectable labeling for *Kcnq1*. In addition, the basal membrane in colonic epithelia from both guinea pig and rat lacked distinct labeling for *Kcnq1*, consistent with a dominant localization only to lateral membranes. Without consistent apical or basal labeling to use as a guide, the possible presence of *Kcnq1* in goblet cells remains equivocal, compared with its likely presence in columnar cells.

The use of the secondary antibody alone eliminated all membrane labeling of epithelial cells observed in rat (Fig. 1*B*) and guinea pig colon (data not shown), indicating that the *Kcnq1* antibody was necessary for the observed labeling. The antigenic peptide was not available for preabsorption of the *Kcnq1* antibody as a further control for nonspecific reactions. An antibody against the metabotropic glutamate receptor was used as an additional control for nonspecific labeling of membrane proteins, but no mucosal labeling was detected with this antibody (data not shown). In perfusion-fixed specimens, the surface epithelium had a diffuse, low-level labeling (Fig. 1*A*), predominantly in the cytoplasm (darker nuclei), which also was evident in the absence of the primary antibody (Fig. 1*B*). The bright cells in the interstitium were probably leukocytes as reported previously, with visibility likely due to autofluorescence of granule contents and nonspecific binding of the secondary antibody (8, 48).

Immunoreactivity for the $K^+$ channel regulatory protein MiRP2, *Kcne3*, was detected in the lateral membrane of guinea pig colonic crypt epithelia (Fig. 3*A*), consistent with previous reports for mouse colon using immunolocalization and patch-clamp recording of channel activity (14, 58). Lateral membranes of surface cells also labeled for *Kcne3* (Fig. 3, *C* and *D*). All of the membrane labeling was eliminated by preabsorption of the primary antibody with the antigenic peptide (Fig. 3*B*). The labeling in crypt and surface epithelial cells occurred with a beaded appearance, suggesting that *Kcne3* clustered at sites along the lateral membrane. Neither apical nor basal membranes in surface cells showed detectable labeling.

The presence of the $K^+$ channel proteins *Kcnq1* and *Kcne3* in the colonic mucosa also was examined using immunoblot analysis (Fig. 4). A membrane sample from rat distal colonic mucosa exhibited an immunoreactive band for *Kcnq1*. Similarly, membrane samples from early and late portions of guinea pig distal colon showed bands of about the same size. The *Kcne3* regulatory subunit also was detected in this membrane sample. These results further support the presence of these two $K^+$ channel proteins in the colonic mucosa.

*Stimulation of secretory modes.* Suppressing endogenous activators enhanced the ability to examine secretory modes in the isolated colonic mucosa by producing a consistent quiescent basal state. The mucosal preparation removes the influence of nerves in the underlying muscle layers such that only mucosal nerves remain (9). Previous studies demonstrated that these mucosal nerves do not contribute to the secretory stimulation by secretagogues (9, 15, 30, 53). The effects of endogenous paracrine activators also were reduced, which aided in producing a basal state (30). Production of prostanoids within the mucosa was limited with the cyclooxygenase (COX) inhibitor indomethacin (2 μM) and COX-2 inhibitor NS-398 (2 μM). Other potentially stimulatory compounds that may have been released from cells in the mucosa were reduced in concentration by replacing the bath solutions three times at ~15-min intervals after mounting the tissues in the chambers (30). This consistent basal state further improved the use of adjacent tissue pairs for interpretation of inhibitor results by limiting variability due to stimulatory status.

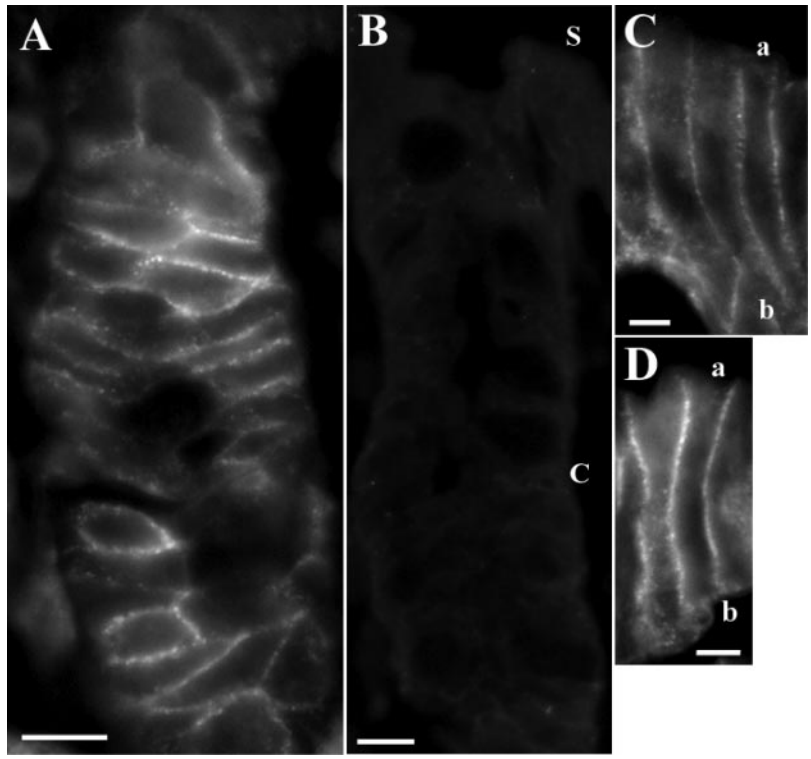


Fig. 3. Localization of minK-related peptide 2 (MiRP2, *Kcne3*) immunoreactivity in guinea pig distal colonic mucosa. *Kcne3* was detected using immunofluorescence in guinea pig distal colonic mucosa fixed after isolation (anti-*Kcne3*-L20; Santa Cruz Biotechnology). *A*: lateral membranes of crypt cells showed distinct labeling. *B*: when the primary antibody was preabsorbed with the antigenic peptide, nonspecific labeling of crypt and surface epithelial cells was low. Epithelial profiles of surface epithelium (*C* and *D*) showed labeling extending along the length of the lateral margin of columnar cells without any labeling in the apical membrane (a) and only weak if any indications of labeling in the basal membrane (b) region. Labeling of mucosa by a distinct antibody for *Kcne3* (anti-*Kcne3*-N18) had a similar appearance (data not shown). Scale bars, 10 μm for *A* and *B*; 5 μm for *C* and *D*.

Distinct secretory states were produced after attaining the basal condition by adding specific secretagogues (30, 53). Sustained electrogenic $K^+$ secretion of the modulatory type was stimulated by addition of either EPI (5 μM) or $PGE_2$ at low concentration (5 nM). Addition of $PGE_2$ at high concentration (3 μM) stimulated flushing-type secretion consisting of sustained $Cl^-$ secretion together with $K^+$ secretion. Adding carbachol (CCh; 10 μM) cumulatively with $PGE_2$ (3 μM) produced a further large synergistic increase in $Cl^-$ secretion with a transient component lasting 10–20 min. Each of these distinct secretory modes was examined for sensitivity to *Kcnq1* inhibitors, including *1*) modulatory-type $K^+$ secretion, *2*) flushing-type $Cl^-$ and $K^+$ secretion, and *3*) synergistic $Cl^-$ secretion.

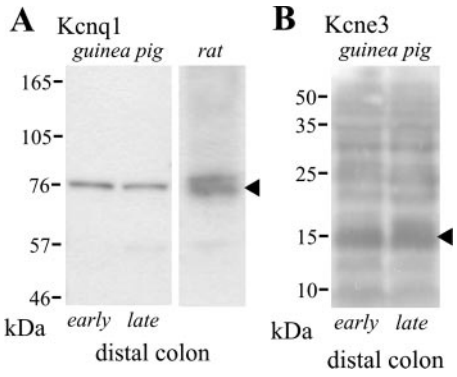


Fig. 4. $K^+$ channel immunoblots. Protein isolated from colonic mucosa of guinea pig and rat were immunoblotted with antibodies against the $K^+$ channel proteins (*A*) *Kcnq1* and (*B*) *Kcne3* (anti-*Kcne3*-L20). Arrowheads indicate bands of the size expected for these proteins (*Kcnq1*, 74 kDa; *Kcne3*, 14 kDa). Preabsorption of the anti-*Kcne3*-L20 antibody with antigenic peptide diminished the distinct band at ~15 kDa for *Kcne3*, whereas the other, fainter bands represent nonspecific interactions of the secondary antibody (0.004 ng/μl donkey anti-goat IgG antibody; Jackson ImmunoResearch).

*Inhibition of secretory modes.* The chromanol 293B has been shown to inhibit the *Kcnq1* $K^+$ channel as well as $Cl^-$ secretion (21, 43, 45, 62, 63). A higher-affinity inhibition of *Kcnq1* is obtained with the 293B derivative HMR1556 (22); from different cell types, the $IC_{50}$ for HMR1556 ranges from 7 to 170 nM (5, 23, 37, 39, 61). In rat colonic mucosa (Fig. 5), HMR1556 (10 μM) inhibited a portion of the flushing-type $Cl^-$-secretory $I_{sc}$ and $G_t$ stimulated by $PGE_2$ but did not alter the modulatory-type $K^+$-secretory $I_{sc}$ and $G_t$ stimulated by EPI. Inhibition was rapid for both $I_{sc}$ and $G_t$. The HMR1556-sensitive component of the $PGE_2$ response reached a maximum within ~10 min and remained stable with only a slight decline over 15 min (Fig. 5*C*). The HMR1556-sensitive and HMR1556-resistant components of the $PGE_2$-secretory response were similar in size.

HMR1556 (10 μM) did not noticeably alter the response of guinea pig distal colonic mucosa to EPI or $PGE_2$ when added to either the serosal bath (Fig. 6) or the mucosal bath (data not shown). The EPI-stimulated modulatory $I_{sc}$ was roughly threefold for the guinea pig compared with the rat, with an indication of only minor inhibition. Even though the $PGE_2$-stimulated flushing $I_{sc}$ was similar for guinea pig and rat, evidence of inhibition was absent for the guinea pig. Increasing the concentration of HMR1556 to 30 μM did not alter the $PGE_2$-stimulated flushing $I_{sc}$ (data not shown). Similarly, the chromanol 293B (100 μM) did not alter significantly the EPI response ($\Delta I_{sc} = 3.5 \pm 3.0$ μA/cm$^2$ and $\Delta G_t = 0.72 \pm 0.71$ mS/cm$^2$; $n = 3$). Serosally added 293B (100 μM), however, produced a significant but modest (~13%) inhibition of the guinea pig flushing response ($\Delta I_{sc} = -15.7 \pm 2.3$ μA/cm$^2$, $\Delta G_t = -1.19 \pm 0.28$ mS/cm$^2$; $n = 3$).

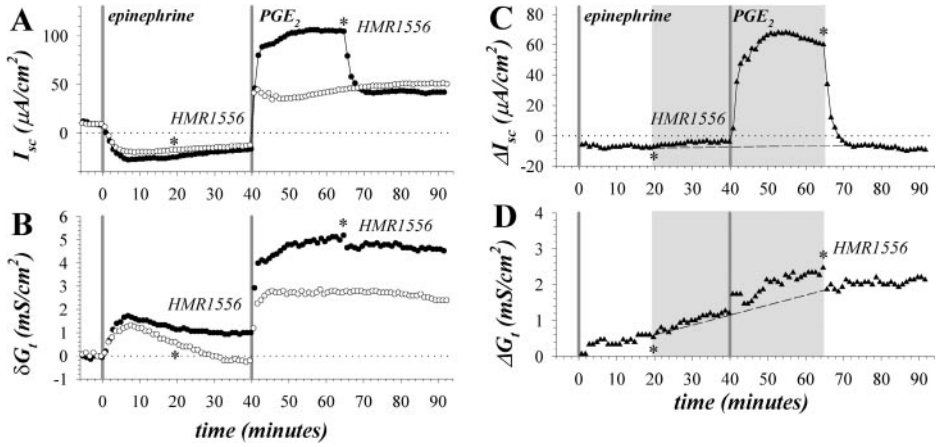


Fig. 5. HMR1556 sensitivity of modulatory and flushing secretion in rat colon. Rat distal colonic mucosae were stimulated cumulatively by epinephrine (EPI; 5 μM) and prostaglandin $E_2$ ($PGE_2$; 3 μM), from the standard basal condition. The basal condition was produced by three successive bath replacements, indomethacin (2 μM) and NS398 (2 μM) in both bathing solutions and amiloride (100 μM) in the mucosal bathing solution. Short-circuit current ($I_{sc}$; *A*) and transepithelial conductance ($G_t$; *B*) are shown. $G_t$ changes shown ($\Delta G_t$) had the prestimulation value subtracted (○, 9.5 mS/cm$^2$; ●, 11.2 mS/cm$^2$). HMR1556 (10 μM) was added to the serosal bath (asterisk) for an adjacent pair of mucosae during stimulation by either EPI (○) or $PGE_2$ (●). Differences within the pair for $I_{sc}$ and $G_t$ (*C* and *D*) revealed the HMR1556-sensitive components (shaded region) of EPI and $PGE_2$ responses. The dashed line connects periods of identical treatment conditions for the tissue pair. The rate of change for $G_t$ in the secretory state was different between the mucosae in this pair, but an abrupt change occurred with HMR1556 addition during $PGE_2$ stimulation.

Modulatory $K^+$ secretion (30) also was stimulated in guinea pig distal colonic mucosa with $PGE_2$ at 5 nM ($\Delta I_{sc} = -71.0 \pm 2.6$ μA/cm$^2$; $n = 6$), followed by an increase of $PGE_2$ to 3 μM that produced flushing secretion ($\Delta I_{sc} = 98.8 \pm 9.7$ μA/cm$^2$; $n = 6$). HMR1556 did not alter significantly either the modulatory ($\Delta I_{sc} = 3.3 \pm 1.9$ μA/cm$^2$, $\Delta G_t = -0.22 \pm 0.18$ mS/cm$^2$; $n = 6$) or the flushing response ($\Delta I_{sc} = 1.2 \pm 5.3$ μA/cm$^2$, $\Delta G_t = 0.21 \pm 0.26$ mS/cm$^2$; $n = 6$). Thus the presence of EPI was not responsible for inducing insensitivity to HMR1556.

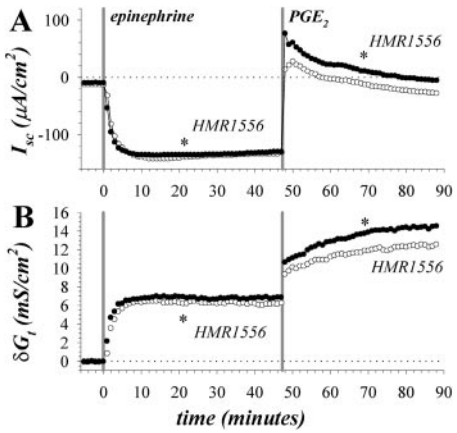


Fig. 6. HMR1556 sensitivity of modulatory and flushing secretion in guinea pig colon. Guinea pig mucosae from late distal colon were stimulated cumulatively by EPI (5 μM) and $PGE_2$ (3 μM) from the standard basal condition as shown in Fig. 5. $I_{sc}$ (*A*) and $G_t$ (*B*) are shown. $G_t$ changes shown ($\Delta G_t$) had the prestimulation value subtracted (○, 12.7 mS/cm$^2$; ●, 11.2 mS/cm$^2$). HMR1556 (10 μM) was added to the serosal bath (asterisk) for an adjacent pair of mucosae during stimulation by either EPI (○) or $PGE_2$ (●). Abrupt changes with HMR1556 were not apparent, and paired HMR1556 responses during EPI ($\Delta I_{sc} = 4.9 \pm 0.8$ μA/cm$^2$, $\Delta G_t = 0.20 \pm 0.24$ mS/cm$^2$; $n = 7$) or $PGE_2$ ($\Delta I_{sc} = 0.9 \pm 4.0$ μA/cm$^2$, $\Delta G_t = -0.18 \pm 0.17$ mS/cm$^2$; $n = 7$) were not significantly different from zero ($P < 0.05$), except for the small (3%) increase in $I_{sc}$ with EPI.

The secretory responses in the rat were dependent on the position along the colon (Fig. 7), with a larger EPI-stimulated, modulatory $K^+$ secretion at more distal sites and a larger $PGE_2$-stimulated, flushing $Cl^-$ secretion at more proximal sites. The $I_{sc}$ and $G_t$ in basal and $PGE_2$ conditions were similar to earlier results found using mucosal preparations of rat distal colon (3, 15). In addition, $G_t$ tended to be larger at proximal sites, similar to findings in earlier studies (33, 57). The $PGE_2$-stimulated $Cl^-$-secretory response was calculated as the difference between the $I_{sc}$ after $PGE_2$ addition and the prior EPI-stimulated $I_{sc}$ to include the full range of secretory capacity (Fig. 7*B*). The HMR1556-sensitive and HMR1556-resistant components of this $PGE_2$-stimulated $Cl^-$-secretory response in rat colon were not different in size at any position examined (Fig. 7, *B* and *C*). The $IC_{50}$ was 55 ± 11 nM for this HMR1556 inhibition of the $PGE_2$-stimulated $Cl^-$-secretory response (Fig. 8). For the guinea pig distal colon, the EPI-stimulated, modulatory $I_{sc}$, and $PGE_2$-stimulated flushing $I_{sc}$ were approximately −100 μA/cm$^2$ and +120 μA/cm$^2$, respectively, in both early and late portions, and the lack of inhibition by HMR1556 also was similar along the length of the distal colon.

Stimulation of synergistic $Cl^-$ secretion by CCh (in the presence of $PGE_2$) in rat colonic mucosa produced a transiently larger $I_{sc}$, followed by a sustained $I_{sc}$ lower than that observed with $PGE_2$ alone (Fig. 9). HMR1556 inhibited the sustained $I_{sc}$ more than the transient $I_{sc}$. The reduction in the HMR1556-sensitive $I_{sc}$ (Fig. 9*C*) after CCh addition indicated that the inhibitory action of CCh on sustained $Cl^-$ secretion resulted in a smaller reliance on *Kcnq1*. The reduction likely occurred at least in part through an inhibition of *Kcnq1* $K^+$ channels, because the total $I_{sc}$ (Fig. 9*A*) was lower after CCh addition than after the addition of $PGE_2$ alone.

High rates of CCh-stimulated $Cl^-$ secretion in isolated colonic mucosa have been shown to occur as a result of endogenous prostanoid production and submucosal nerve activity; treatment of colonic mucosa with indomethacin elimi-

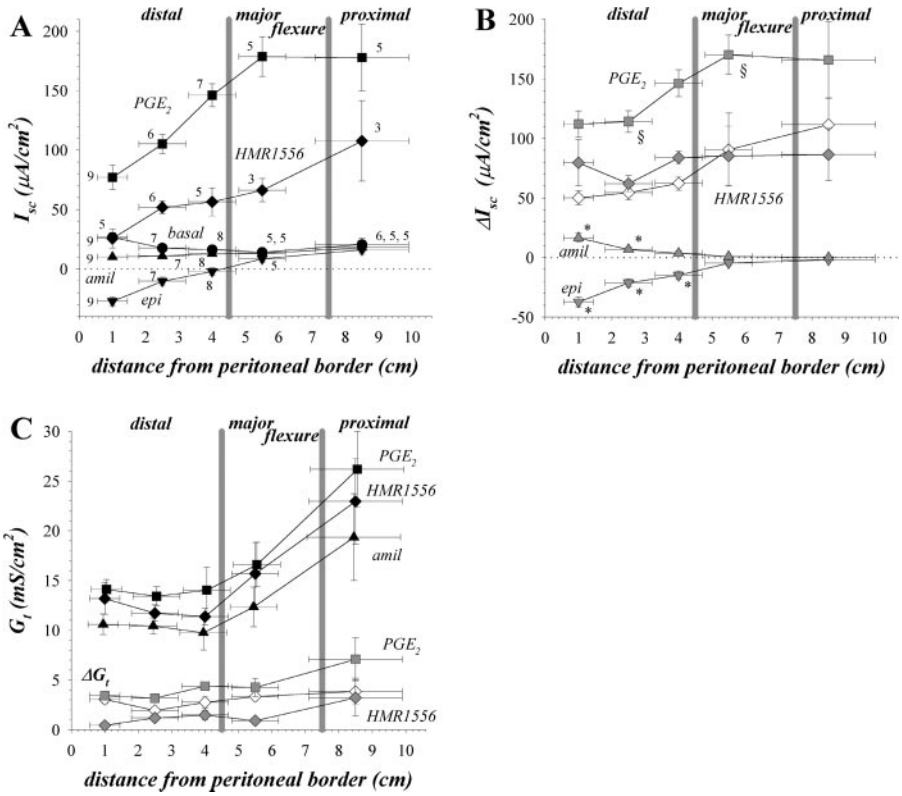


Fig. 7. HMR1556 sensitivity along the proximal-distal axis in rat colon. Rat colonic mucosae were stimulated as in Fig. 5, with HMR1556 added after $PGE_2$-stimulation. $I_{sc}$ and $G_t$ values (means ± SE; N) are shown (*A* and *C*) for positions measured orad from the peritoneal border (●, basal; ▲, amiloride; ▼, EPI; ■, $PGE_2$; ◆, HMR1556); the error bars for position include the chamber aperture (0.9 cm) and an estimate of uncertainty for the position of the mucosal specimen. Paired differences between successive conditions also are shown (*B* and *C*), with the HMR1556-resistant component included (◇). Asterisks (*B*) mark $\Delta I_{sc}$ values for amiloride and EPI additions that are significantly different from zero ($P < 0.05$); all other $\Delta I_{sc}$ are significantly different from zero. The amiloride-sensitive $\Delta I_{sc}$ value at 1.0 cm was significantly different from the value at 2.5 cm ($P < 0.05$), and the EPI-stimulated $\Delta I_{sc}$ values at the three distal positions were significantly different from each other ($P < 0.05$). The $PGE_2$-stimulated $\Delta I_{sc}$ value at 5.5 cm (§) was significantly different from the value at 2.5 cm ($P < 0.05$). $G_t$ values (*C*) in basal, amiloride, and EPI conditions were statistically identical ($P < 0.05$), so only the amiloride values are shown; all $\Delta G_t$ shown were significantly different from zero ($P < 0.05$). The three recognized morphologic regions along the rat colon are proximal, major flexural, and distal, with the proximal region having distinct palm leaf mucosal folds (42). The transition from proximal to major flexure occurs at ~7.5 cm, and the transition from major flexure to distal occurs at ~4.5 cm. The end of the colon and the beginning of the rectum are defined anatomically (42) to occur at the peritoneal border (0.0 cm), whereas functionally this transition to rectal colon occurs ~1 cm orad from the peritoneal border (17, 19). The rat colon also has been divided into ascending and descending portions (18) at ~7 cm.

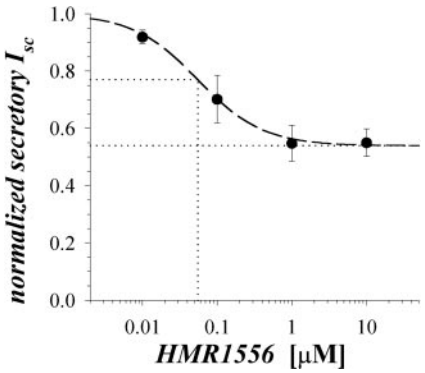


Fig. 8. Concentration-dependent inhibition of flushing secretion by HMR1556. Rat distal colonic mucosae were stimulated as in Fig. 5, followed by cumulative additions of HMR1556 to the $PGE_2$-stimulated state. The HMR1556-resistant proportion of $I_{sc}$ is shown at four concentrations ($n = 5$); the resistant proportion was calculated as $(I_{HMR} - I_{EPI})/(I_{PGE2} - I_{EPI})$. This concentration dependence was not distinctly different along the proximal to distal axis, so results from all positions were included. The $IC_{50}$ was 55 ± 11 nM.

nated sustained $Cl^-$ secretion activated by CCh (10, 46, 60). Guinea pig distal colonic mucosa in a similar basal state showed a sustained negative $I_{sc}$ during CCh stimulation, consistent with modulatory $K^+$ secretion (Fig. 10). Similarly to EPI-stimulated electrogenic $K^+$ secretion (27, 53), bumetanide inhibited this CCh-stimulated negative $I_{sc}$. The $EC_{50}$ for CCh in this modulatory cholinergic response was 1.6 ± 0.4 μM ($n = 3$).

Addition of $PGE_2$ at high concentration to CCh-stimulated guinea pig mucosa produced a large increase in $I_{sc}$ (Fig. 11). This synergistic stimulation of $Cl^-$ secretion by CCh together with $PGE_2$ occurred with an $EC_{50}$ for $PGE_2$ of 93 ± 8 nM ($n = 3$), consistent with action via a novel receptor distinct from the prostanoid EP subtypes (30). HMR1556 did not alter this synergistic response of guinea pig distal colonic mucosa, regardless of whether it was added during CCh stimulation or after $PGE_2$ stimulation. Increasing the concentration of HMR1556 from 10 to 30 μM during $PGE_2$ stimulation also did not alter the secretory response (Fig. 11). However, the chromanol 293B (100 μM) produced a significant but modest (~13%) inhibition of this large synergistic CCh/$PGE_2$ re-

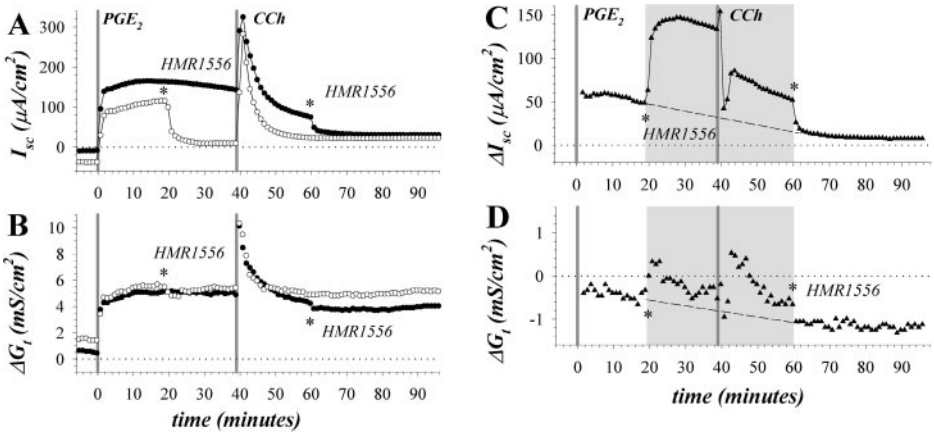


Fig. 9. HMR1556 sensitivity of cholinergic response in rat colon. Rat distal colonic mucosae were stimulated as in Fig. 5, followed by carbachol (CCh; 10 μM) addition (*A* and *B*). $G_t$ changes ($\Delta G_t$) shown had the prestimulation value subtracted (○, 7.3 mS/cm$^2$; ●, 9.1 mS/cm$^2$). HMR1556 (10 μM) was added to the serosal bath (asterisk) for an adjacent pair of mucosae during stimulation by either $PGE_2$ (○) or CCh (●). Differences within the pair for $I_{sc}$ and $G_t$ (*C* and *D*) revealed the HMR1556-sensitive components (shaded region) of $PGE_2$ and CCh responses. The dashed line connects periods of identical treatment conditions for the tissue pair.

sponse ($\Delta I_{sc} = -51.6 \pm 11.1$ μA/cm$^2$, $\Delta G_t = -1.06 \pm 0.23$ mS/cm$^2$; $n = 3$).

The influence of HMR1556 on the activation time course for $PGE_2$-stimulated flushing secretion was consistent with the initiation of a two-stage process (Fig. 12, *A* and *B*). As shown by the average $PGE_2$ responses, the first phase of activation was rapid, lasting ~40 s, and was similar for control and treated mucosae. The responses then diverged, with control mucosae reaching an approximately twofold higher steady-state $I_{sc}$ during the next 3 min. In the presence of HMR1556, $I_{sc}$ oscillated in an underdamped fashion for ~10 min, with a period of ~2.3 min. The average synergistic activation by CCh (Fig. 12, *C* and *D*) indicated an inhibitory action on the HMR-sensitive $I_{sc}$ such that this secretory mode must rely primarily on $K^+$ channels other than *Kcnq1*.

## DISCUSSION

In colonic epithelia, $K^+$ channels have clear roles in developing the electrochemical gradients that drive ion flows across the apical and basolateral membranes (24, 26, 27, 63). The $K^+$ channels that are located in the basolateral membrane support all of the transepithelial flows dependent on $Na^+$-$K^+$-ATPase, including electrogenic $Na^+$ absorption and $Cl^-$ secretion. Basolateral membrane $K^+$ channels also may contribute directly to the transcellular pathway for $K^+$ absorption that is driven by apical membrane $H^+$-$K^+$-ATPase. Similarly, the presence of $K^+$ channels in the apical membrane provides an exit route for $K^+$ taken up by basolateral membrane $Na^+$-$K^+$-ATPase, which immediately results in electrogenic $K^+$ secretion. Identifying the $K^+$ channel types involved in each of the transport functions present in the colonic epithelium would allow a more complete definition of these long-studied cellular transport mechanisms. Specifying the particular $K^+$ channels is not a simple task, given the large number of genes encoding $K^+$ channel proteins and auxiliary subunits (1, 13, 35, 49, 55), but identification of the subunits involved would provide a more direct means by which to assess the regulatory cascades that control channel activity.

Voltage-sensitive $K^+$ channels ($K_V$) are not obvious choices as components of epithelial transport mechanisms, because changes in membrane electrical potential differences are rela-

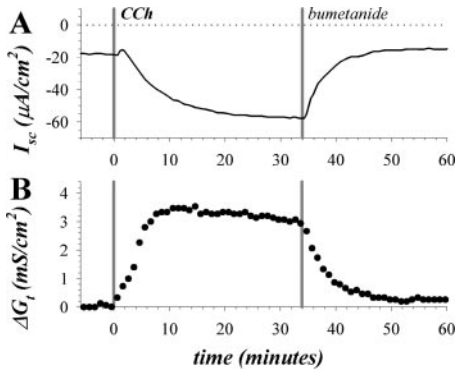


Fig. 10. Cholinergic stimulation of electrogenic $K^+$ secretion in guinea pig colon. Guinea pig mucosae from late distal colon were stimulated with CCh (10 μM), from the standard basal condition as shown in Fig. 5. $I_{sc}$ (*A*) and $G_t$ (*B*) from a representative mucosa are shown. $G_t$ changes ($\Delta G_t$) shown had the prestimulation value subtracted (8.2 mS/cm$^2$). Bumetanide (100 μM) was added to the serosal bath. Average CCh-stimulated $\Delta I_{sc}$ was $-47.8 \pm 3.9$ μA/cm$^2$, and mean $\Delta G_t$ was $3.20 \pm 0.23$ mS/cm$^2$ ($n = 15$).

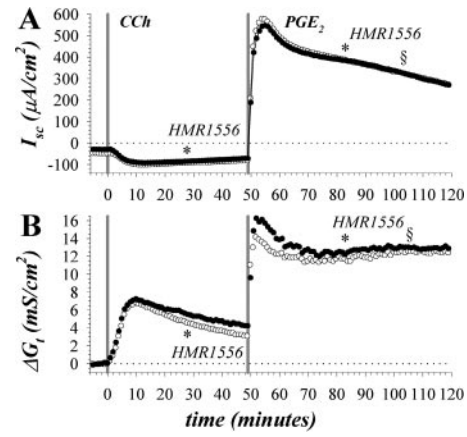


Fig. 11. HMR1556 sensitivity of the cholinergic modulatory and synergistic responses in guinea pig colon. Guinea pig mucosae from late distal colon (*A* and *B*) were stimulated cumulatively by CCh (10 μM) and $PGE_2$ (3 μM) from the standard basal condition as shown in Fig. 5. $G_t$ changes ($\Delta G_t$) shown had the prestimulation value subtracted (○, 8.6 mS/cm$^2$; ●, 9.8 mS/cm$^2$). HMR1556 (10 μM) was added to the serosal bath (asterisk) for an adjacent pair of mucosae during stimulation by either CCh (○) or $PGE_2$ (●). Subsequently, HMR1556 concentration was increased to 30 μM (§) for one mucosa of the pair (●). Abrupt changes with HMR1556 were not apparent, and paired HMR1556 responses during CCh ($\Delta I_{sc} = -0.7 \pm 3.2$ μA/cm$^2$, $\Delta G_t = -0.14 \pm 0.38$ mS/cm$^2$; $n = 4$) or CCh/$PGE_2$ ($\Delta I_{sc} = 6.0 \pm 9.3$ μA/cm$^2$, $\Delta G_t = -0.61 \pm 0.89$ mS/cm$^2$; $n = 4$) were not significantly different from zero ($P < 0.05$).

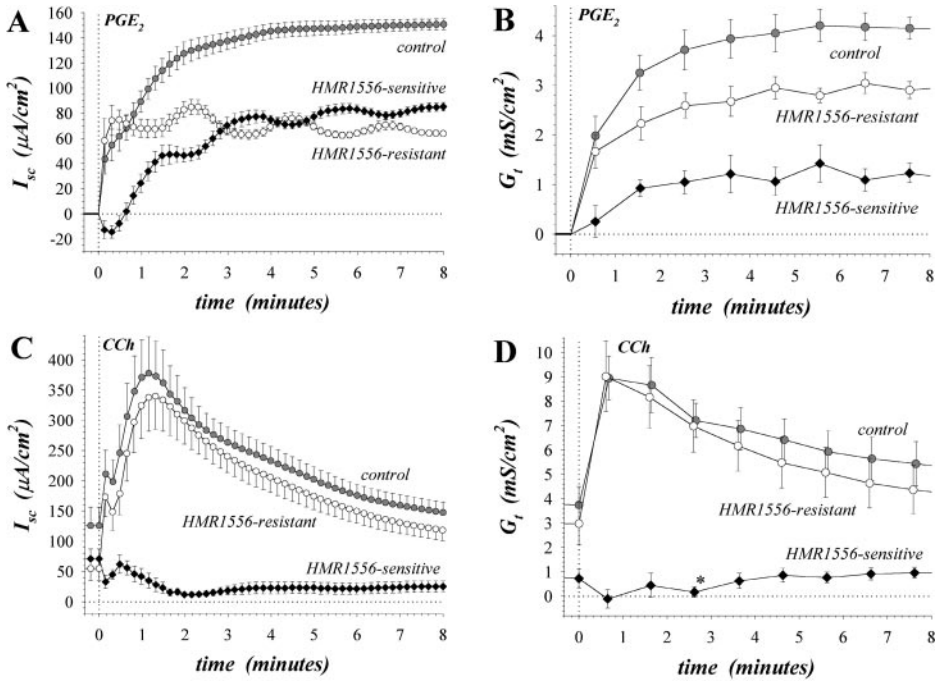


Fig. 12. HMR1556 sensitivity of flushing and synergistic activation in rat colon. Rat distal colonic mucosae were stimulated (as in Fig. 5) by EPI (5 μM), followed by $PGE_2$ (3 μM) at *time 0* (*A* and *B*). Average $PGE_2$-stimulated $I_{sc}$ (*A*) and $G_t$ (*B*) are shown ($n = 5$) for control stimulation (●), with HMR1556 (10 μM) (○) and for the paired difference values between these conditions (◆). SE values were calculated from traces normalized to the maximal response for indication of time course variability; comparisons of maximal responses are in Fig. 7. The half-times for $I_{sc}$ activation ($n = 5$) were 40.4 ± 11.2 s for control, 6.3 ± 2.3 s for the HMR-resistant component, and 80.5 ± 15.6 s for the HMR-sensitive component. Paired mucosae ($n = 6$) also were stimulated (as shown in Fig. 9) with CCh (10 μM) added at *time 0* (*C* and *D*), including control stimulation (●), with HMR1556 (10 μM) (○) and the difference values between these conditions (◆). The starting condition for *C* and *D* was the same as the final condition shown in *A* and *B*. SE values were calculated without normalization. All of the HMR-sensitive $I_{sc}$ (*C*) at times >1.4 min were significantly different from the value before CCh stimulation. Asterisk in *D* indicates a time point at which HMR1556-sensitive $G_t$ was significantly different from the value before CCh stimulation. The minimum HMR-sensitive $I_{sc}$ values at ~2 min of activation were significantly different from zero, as were the maximal values at ~8 min; the maximal HMR-sensitive $G_t$ at ~8 min of activation also was significantly different from zero.

tively modest compared with other cell types, such as neurons and muscle cells. However, in addition to voltage-dependent gating, other signaling cascades regulate many of the $K_V$ channels. In particular, $K_V$LQT1 (*Kcnq1*) is activated by cAMP-dependent mechanisms (36, 55, 58, 65), possibly acting through protein kinase A, and has been shown by several means to contribute to the basolateral membrane $K^+$ conductance necessary for electrogenic $Cl^-$ secretion. The presence in the colon of the mRNA encoding *Kcnq1* was shown using Northern blot analysis (14, 65), and in situ hybridization confirmed that colonic crypt epithelial cells contained this message (58). With the use of rat crypt epithelial cells, previous investigators obtained a full-length cDNA (669 amino acids) of *Kcnq1* that was 90% identical to the amino acid sequence for human *Kcnq1* (36). The involvement of *Kcnq1* in $Cl^-$ secretion was demonstrated using the chromanol 293B that inhibits both *Kcnq1*-dependent currents (6, 36, 58), as well as a current component in rat colonic crypt cells and transepithelial electrogenic $Cl^-$ secretion in rat and mouse colon (36, 43, 45, 58, 62).

Immunofluorescence labeling of mouse colon for *Kcnq1* supports a presence of this $K^+$ channel in the lateral membrane of crypt epithelial cells (14, 62). Similarly, guinea pig and rat colon showed lateral membrane localization of *Kcnq1* immunoreactivity (Figs. 1 and 2). Although nonspecific staining obscured detection of *Kcnq1* in surface epithelial cells of perfusion-fixed rat colon, the low background staining in isolation-fixed guinea pig and rat mucosa allowed a clear determination that *Kcnq1* also was localized to the lateral membrane of surface epithelial cells (Figs. 1 and 2). Further support for the presence of *Kcnq1* in surface epithelial cells was indicated using RT-PCR to detect *Kcnq1* mRNA in rat colonic surface cells (36). Similar to results in other studies of colonic mucosa (14, 36, 58), *Kcnq1* was present together with MiRP2 (*Kcne3*) (Fig. 3), an auxiliary subunit that modifies gating kinetics and inhibitor sensitivity (6, 36, 49, 55, 58). Of course the mere localization of both *Kcnq1* and *Kcne3* to the same membrane using immunofluorescence does not prove a functional connection. However, 293B-sensitive currents have been measured in rat colonic crypt cells with properties similar to defined *Kcnq1*/*Kcne3* currents (36, 63), such that these two $K^+$ channel subunits likely combine to form a component of lateral membrane $K^+$ conductance. Also, the low $IC_{50}$ for HMR1556 (Fig. 8) supports the involvement of *Kcnq1*/*Kcne3* rather than *Kcnq1* alone (39). The additional finding of both *Kcnq1* and *Kcne3* in lateral membranes of colonic surface epithelial cells (Figs. 2 and 3) suggests that these two subunits also combine at this location to produce the weakly voltage-dependent $K^+$ channel characteristic of *Kcnq1*/*Kcne3*. Thus the presence of this $K^+$ channel type does not distinguish surface cells from crypt cells, but perhaps instead a distinction between these cell types occurs at the level at which signaling pathways activate these channels to augment $K^+$ flow.

Ion transport characteristics vary along the length of the colon with amiloride-sensitive $Na^+$ absorption occurring predominantly at distal sites (18, 52, 54). A similar gradient of amiloride-sensitive $I_{sc}$ was detected in this study (Fig. 7*B*). The response to physiological secretagogues also was examined and showed a gradient along the length of the rat colon. The $I_{sc}$ stimulated by the flushing secretagogue $PGE_2$ was ~40% higher at proximal positions compared with more distal positions. For stimulation by the modulatory secretagogue EPI, a sustained $I_{sc}$ was apparent only at distal positions. These results are consistent with an earlier study in which the investigators used a mucosal-submucosal preparation (33), except that the basal $I_{sc}$ was generally higher (by 20–50 $\mu A/cm^2$) than in the present study (Fig. 7*A*), suggesting a difference in secretory status.

The modulatory mode of secretion, characterized by sustained electrogenic $K^+$ secretion without sustained $Cl^-$ secretion, may be considered the most fundamental secretory mode in the distal colon. This concept is supported by experiments in which colonic mucosa were stimulated after the secretory influences from nerves and endogenous production of paracrine factors were first reduced. Stimulation from a quiescent basal state by β-adrenergic (27, 53, 64) (Figs. 5 and 6), prostanoid EP2 subtype (30, 53), and cholinergic agonists (10, 46) (Figs. 10 and 11) all result in modulatory $K^+$ secretion. In addition, stimulation with a low concentration of forskolin, which activates adenylyl cyclase to produce cAMP, also leads to modulatory secretion (41), consistent with the action of β-adrenergic and EP2 prostanoid receptors to increase cellular cAMP. The cholinergic activation of modulatory secretion from a quiescent state (Fig. 10) indicates that other second messengers also are capable of activating this secretory mode and indicates that a distinct secretory state exists compared with the cholinergically induced reduction in flushing-mode $K^+$ secretion of rabbit distal colon (16).

Addition of the lipid-soluble 293B or HMR1556 could block either apical or basolateral $K^+$ channels, but the localization of *Kcnq1* to the basolateral membrane (Figs. 1 and 2) suggests that these inhibitors would act to enhance modulatory $K^+$ secretion by diverting $K^+$ exit to the apical membrane. Because neither HMR1556 nor 293B altered the modulatory response (Figs. 5, 6, and 11) similarly to results with 293B in human and cystic fibrosis mouse colon (45, 47), *Kcnq1* appears to be largely inactive during the modulatory mode of secretion.

Flushing secretion is driven by electrogenic $Cl^-$ secretion, together with an accompanying electrogenic $K^+$ secretion, and is elicited by several types of secretagogues. In particular, $PGE_2$ is produced within the mucosa and at high concentration activates the flushing mode via receptors distinct from the EP prostanoid type (30). The regulatory mechanism stimulating flushing secretion likely involves cAMP because at high concentration forskolin produces large $Cl^-$-secretory $I_{sc}$ (11, 50). In the guinea pig distal colon, increasing forskolin concentration reverses a negative $I_{sc}$ to a positive $I_{sc}$, which is indicative of conversion from modulatory secretion to flushing secretion (41). The flushing-type $Cl^-$-secretory $I_{sc}$ stimulated in colonic mucosa from human (46), mouse (45, 62), rabbit (43), and rat (36, 64) by either forskolin or inhibitors of phosphodiesterase was inhibited from 60 to 90% with the chromanol 293B. In rabbit distal colon, flushing secretion produced by the secretagogues $PGE_2$, adenosine, and vasoactive intestinal peptide was inhibited 70–80% by 293B (43).

A difficulty with assigning a quantitatively specific role for *Kcnq1* on the basis of 293B inhibition is that 293B also inhibits the $Cl^-$ channel CFTR with an $IC_{50}$ of 20–30 μM (4). Because CFTR is a component of the apical $Cl^-$ conductance needed for $Cl^-$ secretion (50), the potency of 293B may result from action at both secretory $K^+$ and $Cl^-$ conductance. The chromanol derivative HMR1556 inhibits *Kcnq1* with ~100-fold higher affinity than 293B (22, 23), such that any similar nonspecificity would not be encountered at concentrations sufficient to inhibit *Kcnq1*. In addition, the dose-response curve of $Cl^-$-secretory $I_{sc}$ in rat colon (Fig. 8) did not include an inflection that would be consistent with such a high concentration inhibitory effect on CFTR. Thus the ~50% inhibition of flushing-type secretion by HMR1556 (Figs. 5 and 7) in rat colon strongly supports a limited requirement for *Kcnq1* $K^+$ channels and the need for at least one other $K^+$ channel type. The lack of inhibition by HMR1556 in guinea pig distal colon (Fig. 6) was not due to the insensitivity of guinea pig *Kcnq1*, because HMR1556 blocks *Kcnq1* currents in guinea pig cardiomyocytes (5, 23). This failure further indicates that flushing secretion could occur without the involvement of *Kcnq1* as part of the basolateral membrane $K^+$ conductance.

The activation time course for flushing secretion in rat colon (Fig. 12, *A* and *B*) supports the concept that *Kcnq1* was needed to produce the slower-onset, secondary phase of secretory capacity. In contrast, the flushing response in guinea pig colon (Fig. 6) had a rapid onset resembling the HMR-resistant component observed in rat colon. Because *Kcnq1* was present in the epithelial cells of guinea pig colonic mucosa, the signaling elicited by $PGE_2$ in these cells apparently lacked regulatory pathways to produce this secondary phase of flushing secretion. Another major difference with rat colon is the higher relative rate of $K^+$ secretion during $PGE_2$ stimulation in the guinea pig colon (53), such that apical membrane $K^+$ channels may satisfy the requirements for additional $K^+$ conductance needed to support high rates of $Cl^-$ secretion.

The present results using the *Kcnq1*/*Kcne3* inhibitor HMR1556 support the concept that distinct $K^+$ channels are needed to produce the secretory modes activated by different types of secretagogues (24). However, the results also indicate that a single type of $K^+$ channel would not be sufficient to produce $Cl^-$ secretion via the ubiquitous flushing secretagogue $PGE_2$. Other studies have indicated that the possible involvement of *Kcnq1* may not be apparent until additional $K^+$ channel types are inhibited (44). However, those observations still suggest that *Kcnq1* apparently is not the preferred $K^+$ channel for activation by those secretagogues. This concept that the secretory cells have a reserve capacity for the activation of $K^+$ channels able to support secretion is underscored by the large $Cl^-$-secretory currents (300–500 $\mu A/cm^2$) that are possible without the need for *Kcnq1* (Figs. 11 and 12). The presence of *Kcnq1* in colonic epithelial cells could serve requirements for cell volume regulation (25) as well as secretory needs. The early oscillatory behavior of the HMR-resistant response (Fig. 12*A*) may represent a volume instability of these secretory cells in attempting to initiate the *Kcnq1*-dependent secondary phase of secretion. Thus the choices that epithelial cells make with regard to which type of $K^+$ channel to activate

during secretion may depend on advantages conveyed by the specific activation and kinetic details of each channel type.


## GRANTS

This study was supported by National Institute of Diabetes and Digestive and Kidney Diseases Grants DK-39007 and DK-65845 and the Wright State University Research Challenge Program.


## REFERENCES


1. **Abbott GW and Goldstein SAN.** $K^+$ channel subunits encoded by the *KCNE* gene family: physiology and pathophysiology of the MinK-related peptides (MiRPs). *Mol Interv* 1: 95–107, 2001.
2. **Allan VJ (ed.).** *Protein Localization by Fluorescence Microscopy*: *A Practical Approach*. Oxford, UK: Oxford University, 2000.
3. **Andres H, Rock R, Bridges RJ, Rummel W, and Schreiner J.** Submucosal plexus and electrolyte transport across rat colonic mucosa. *J Physiol* 364: 301–312, 1985.
4. **Bachmann A, Quast U, and Russ U.** Chromanol 293B, a blocker of the slow delayed rectifier $K^+$ current ($I_{Ks}$), inhibits the CFTR $Cl^-$ current. *Naunyn Schmiedebergs Arch Pharmacol* 363: 590–596, 2001.
5. **Bosch RF, Schneck AC, Csillag S, Eigenberger B, Gerlach U, Brendel J, Lang HJ, Mewis C, Gögelein H, Seipel L, and Kühlkamp V.** Effects of the chromanol HMR 1556 on potassium currents in atrial myocytes. *Naunyn Schmiedebergs Arch Pharmacol* 367: 281–288, 2003.
6. **Boucherot A, Shreiber R, and Kunzelmann K.** Regulation and properties of KCNQ1 ($K_V$LQT1) and impact of the cystic fibrosis transmembrane conductance regulator. *J Membr Biol* 182: 39–47, 2001.
7. **Bradford M.** A rapid and sensitive method for the quantification of microgram quantities of proteins utilizing the principle of protein-dye binding. *Anal Biochem* 72: 248–254, 1976.
8. **Brandtzaeg P.** Immunofluorescence studies of mucous membranes and exocrine glands. In: *Immunofluorescence Technology*: *Selected Theoretical and Clinical Aspects*, edited by Wick G, Traill KN, and Schauenstein K. New York: Elsevier, 1982, p. 167–217.
9. **Bridges RJ, Rack M, Rummel W, and Schreiner J.** Mucosal plexus and electrolyte transport across the rat colonic mucosa. *J Physiol* 376: 531–542, 1986.
10. **Carew MA and Thorn P.** Carbachol-stimulated $Cl^-$ secretion in mouse colon: evidence of a role for autocrine prostaglandin-$E_2$ release. *Exp Physiol* 85: 67–72, 2000.
11. **Chang EB and Rao MC.** Intestinal water and electrolyte transport: mechanisms of physiological and adaptive responses. *Physiology of the Gastrointestinal Tract* (3rd ed.), edited by Johnson LR. New York: Raven, 1994, vol. 2, p. 2027–2081.
12. **Chang WWL and Leblond CP.** Renewal of the epithelium in the descending colon of the mouse: I. Presence of three cell populations: vacuolated-columnar, mucous and argentaffin. *Am J Anat* 131: 73–99, 1971.
13. **Coetzee WA, Amarillo Y, Chiu J, Chow A, Lau D, McCormack T, Morena H, Nadal MS, Ozaita A, Pountney D, Saganich M, Vega-Saenz de Miera E, and Rudy B.** Molecular diversity of $K^+$ channels. *Ann NY Acad Sci* 868: 233–285, 1999.
14. **Dedek K and Waldegger S.** Colocalization of KCNQ1/KCNE channel subunits in the mouse gastrointestinal tract. *Pflügers Arch* 442: 896–902, 2001.
15. **Diener M, Bridges RJ, Knobloch SF, and Rummel W.** Neuronally mediated and direct effects of prostaglandins on ion transport in rat colon descendens. *Naunyn Schmiedebergs Arch Pharmacol* 337: 74–78, 1988.
16. **Freel RW, Vaziri ND, and Hatch M.** Muscarinic down-regulation of cAMP-stimulated potassium ion secretion by rabbit distal colon. *Pflügers Arch* 440: 243–252, 2000.
17. **Fromm M and Hegel U.** Net ion fluxes and zero flux limiting concentrations in rat upper colon and rectum during anaesthesia-induced aldosterone liberation. *Pflügers Arch* 408: 185–193, 1987.
18. **Fromm M, Hegel U, and Lüderitz S.** Segmental heterogeneity of epithelial transport in rat large intestine. *Pflügers Arch* 378: 71–83, 1978.
19. **Fromm M, Schulzke JD, and Hegel U.** Aldosterone low-dose, short-term action in adrenalectomized glucocorticoid-substituted rats: $Na^+$, $K^+$, $Cl^-$, $HCO_3^-$, osmolyte, and water transport in proximal and rectal colon. *Pflügers Arch* 416: 573–579, 1990.
20. **Geiman EJ, Zheng W, Fritschy JM, and Alvarez FJ.** Glycine and $GABA_A$ receptor subunits on Renshaw cells: relationship with presynaptic neurotransmitters and postsynaptic gephyrin clusters. *J Comp Neurol* 444: 275–289, 2002.
21. **Gerlach U.** $I_{Ks}$ channel blockers: potential antiarrhythmic agents. *Drugs Future* 26: 473–484, 2001.
22. **Gerlach U, Brendel J, Lang HJ, Paulus EF, Weidmann K, Brüggemann A, Busch A, Suessbrich H, Bleich M, and Greger R.** Synthesis and activity of novel and selective $I_{Ks}$-channel blockers. *J Med Chem* 44: 3831–3837, 2001.
23. **Gögelein H, Brüggemann A, Gerlach U, Brendel J, and Busch AE.** Inhibition of $I_{Ks}$ channels by HMR1556. *Naunyn Schmiedebergs Arch Pharmacol* 362: 480–488, 2000.
24. **Greger R, Bleich M, Riedemann N, van Driessche W, Ecke D, and Warth R.** The role of $K^+$ channels in colonic $Cl^-$ secretion. *Comp Biochem Physiol A Physiol* 118: 271–275, 1997.
25. **Grunnet M, Jespersen T, MacAulay N, Jørgensen NK, Schmitt N, Pongs O, Olesen SP, and Klaerke DA.** KCNQ1 channels sense small changes in cell volume. *J Physiol* 549: 419–427, 2003.
26. **Halm DR and Frizzell RA.** Intestinal chloride secretion. In: *Textbook of Secretory Diarrhea*, edited by Lebenthal E and Duffey ME. New York: Raven, 1990, p. 47–58.
27. **Halm DR and Frizzell RA.** Ion transport across the large intestine. In: *Handbook of Physiology. The Gastrointestinal System. Intestinal Absorption and Secretion*. Bethesda, MD: Am. Physiol. Soc., 1991, sect. 6, vol. IV, chapt. 8, p. 257–274.
28. **Halm DR and Halm ST.** Secretagogue response of goblet cells and columnar cells in human colonic crypts. *Am J Physiol Cell Physiol* 277: C501–C522, 1999.
29. **Halm DR, Halm ST, DiBona DR, Frizzell RA, and Johnson RD.** Selective stimulation of epithelial cells in colonic crypts: relation to active chloride secretion. *Am J Physiol Cell Physiol* 269: C929–C942, 1995.
30. **Halm DR and Halm ST.** Prostanoids stimulate K secretion and Cl secretion in guinea pig distal colon via distinct pathways. *Am J Physiol Gastrointest Liver Physiol* 281: G984–G996, 2001.
31. **Halm DR, Kirk KL, and Sathiakumar KC.** Stimulation of Cl permeability in colonic crypts of Lieberkühn measured with a fluorescent indicator. *Am J Physiol Gastrointest Liver Physiol* 265: G423–G431, 1993.
32. **Halm DR and Rick R.** Secretion of K and Cl across colonic epithelium: cellular localization using electron microprobe analysis. *Am J Physiol Cell Physiol* 262: C1392–C1402, 1992.
33. **Hörger S, Schulteiss G, and Diener M.** Segment-specific effects of epinephrine on ion transport in the colon of the rat. *Am J Physiol Gastrointest Liver Physiol* 275: G1367–G1376, 1998.
34. **Joiner WJ, Basavappa S, Vidyasagar S, Nehrke K, Krishnan S, Binder HJ, Boulpaep EL, and Rajendran VM.** Active $K^+$ secretion through multiple $K_{Ca}$-type channels and regulation by $IK_{Ca}$ channels in rat proximal colon. *Am J Physiol Gastrointest Liver Physiol* 285: G185–G196, 2003.
35. **Kubo Y.** Overview of $K^+$ channel families: molecular bases of the functional diversity. In: *Handbook of Experimental Pharmacology. Pharmacology of Ionic Channel Function. Activators and Inhibitors*, edited by Endo M, Kurachi Y, and Mishina M. Berlin, Germany: Springer, 2000, vol. 147, p. 157–176.
36. **Kunzelmann K, Hübner M, Schreiber R, Levy-Holzman R, Garty H, Bleich M, Warth R, Slavik M, von Hahn T, and Greger R.** Cloning and function of the rat colonic epithelial $K^+$ channel $K_V$LQT1. *J Membr Biol* 179: 155–164, 2001.
37. **Lee JE, Gerlach U, Uhm DY, and Kim SJ.** Inhibitory effect of somatostatin on secretin-induced augmentation of the slowly activating $K^+$ current ($I_{Ks}$) in the rat pancreatic acinar cell. *Pflügers Arch* 443: 405–410, 2002.
38. **Lee JE, Park HS, Uhm DY, and Kim SJ.** Effects of KCNQ1 channel blocker, 293B, on the acetylcholine-induced $Cl^-$ secretion of rat pancreatic acini. *Pancreas* 28: 435–442, 2004.
39. **Lerche C, Seebohm G, Wagner CI, Scherer CR, Dehmelt L, Abitbol I, Gerlach U, Brendel J, Attali B, and Busch AE.** Molecular impact of MinK on the enantiospecific block of $I_{Ks}$ by chromanols. *Br J Pharmacol* 131: 1503–1506, 2000.
40. **Li Y and Halm DR.** Secretory modulation of basolateral membrane inwardly rectified $K^+$ channel in guinea pig distal colonic crypts. *Am J Physiol Cell Physiol* 282: C719–C735, 2002.
41. **Li Y, Halm ST, and Halm DR.** Secretory activation of basolateral membrane $Cl^-$ channels in guinea pig distal colonic crypts. *Am J Physiol Cell Physiol* 284: C918–C933, 2003.

42. **Lindström CG, Rosengren JE, and Fork FT.** Colon of the rat: an anatomic, histologic and radiographic investigation. *Acta Radiol Diagn (Stockh)* 20: 523–536, 1979.
43. **Lohrmann E, Burhoff I, Nitschke RB, Lang HJ, Mania D, Englert HC, Hropot M, Warth R, Rohm W, Bleich M, and Greger R.** A new class of inhibitors of cAMP-mediated $Cl^-$ secretion in rabbit colon, acting by the reduction of cAMP-activated $K^+$ conductance. *Pflügers Arch* 429: 517–530, 1995.
44. **MacVinish LJ, Guo Y, Dixon AK, Murrell-Lagnado RD, and Cuthbert AW.** XE991 reveals differences in $K^+$ channels regulating $Cl^-$ secretion in murine airway and colonic epithelium. *Mol Pharmacol* 60: 753–760, 2001.
45. **MacVinish LJ, Hickman ME, Mufti DAH, Durrington HJ, and Cuthbert AW.** Importance of basolateral $K^+$ conductance in maintaining $Cl^-$ secretion in murine nasal and colonic epithelia. *J Physiol* 510: 237–247, 1998.
46. **Mall M, Bleich M, Schürlein M, Kühr J, Seydewitz HH, Brandis M, Greger R, and Kunzelmann K.** Cholinergic ion secretion in human colon requires coactivation by cAMP. *Am J Physiol Gastrointest Liver Physiol* 275: G1274–G1281, 1998.
47. **Mall M, Wissner A, Seydewitz HH, Kühr J, Brandis M, Greger R, and Kunzelmann K.** Defective cholinergic $Cl^-$ secretion and detection of $K^+$ secretion in rectal biopsies from cystic fibrosis patients. *Am J Physiol Gastrointest Liver Physiol* 278: G617–G624, 2000.
48. **McCarn K, Yursik B, Halim S, and Roche JK.** Peri-epithelial origin of prostanoids in the human colon. *J Cell Physiol* 194: 176–185, 2002.
49. **Melman YF, Krummerman A, and McDonald TV.** KCNE regulation of $K_V$LQT1 channels: structure-function correlates. *Trends Cardiovasc Med* 12: 182–187, 2002.
50. **Montrose MH, Keely SJ, and Barrett KE.** Electrolyte secretion and absorption: small intestine and colon. In: *Textbook of Gastroenterology* (4th ed.), edited by Yamada T. Philadelphia, PA: Lippincott Williams & Wilkins, 2003, vol. 1, p. 308–340.
51. **Pascal RR, Kaye GI, and Lane N.** Colonic pericryptal fibroblast sheath: Replication, migration and cytodifferentiation of a mesenchymal cell system in adult tissue: I. autoradiographic studies of normal rabbit colon. *Gastroenterology* 54: 835–851, 1968.
52. **Rajendran VM and Binder HJ.** Ion transport in rat colon. In: *Ion Transport in Vertebrate Colon*, edited by Clauss W. Berlin, Germany: Springer-Verlag, 1993, p. 113–137.
53. **Rechkemmer G, Frizzell RA, and Halm DR.** Active $K^+$ transport across guinea pig distal colon: Action of secretagogues. *J Physiol* 493: 485–502, 1996.
54. **Rechkemmer G and von Engelhardt W.** Absorption and secretion of electrolytes and short-chain fatty acids in the guinea pig large intestine. In: *Ion Transport in Vertebrate Colon*, edited by Clauss W. Berlin, Germany: Springer-Verlag, 1993, p. 139–167.
55. **Robbins J.** KCNQ $K^+$ channels: physiology, pathophysiology and pharmacology. *Pharmacol Ther* 90: 1–19, 2001.
56. **Sand P and Rydqvist B.** The low conductance $K^+$ channel in human colonic crypt cells has a voltage-dependent permeability not affected by $Mg^{++}$. *Life Sci* 71: 855–864, 2002.
57. **Sandle GI and McGlone F.** Segmental variability of membrane conductances in rat and human colonic epithelia: implications for $Na^+$, $K^+$ and $Cl^-$ transport. *Pflügers Arch* 410: 173–180, 1987.
58. **Schroeder BC, Waldegger S, Fehr S, Bleich M, Warth R, Greger R, and Jentsch TJ.** A constitutively open $K^+$ channel formed by KCNQ1 and KCNE3. *Nature* 403: 196–199, 2000.
59. **Specian RD and Oliver MG.** Functional biology of intestinal goblet cells. *Am J Physiol Cell Physiol* 260: C183–C193, 1991.
60. **Strabel D and Diener M.** Evidence against direct activation of $Cl^-$ secretion by carbachol in the rat distal colon. *Eur J Pharmacol* 274: 181–191, 1995.
61. **Volders PGA, Stengl M, van Opstal JM, Gerlach U, Spätjens RL-HMG, Beekman JDM, Sipido KR, and Vos MA.** Probing the contribution of $I_{Ks}$ to canine ventricular repolarization: key role for β-adrenergic receptor stimulation. *Circulation* 107: 2753–2760, 2003.
62. **Warth R, Alzamora MG, Kim JK, Zdebik A, Nitschke R, Bleich M, Gerlach U, Barhanin J, and Kim SJ.** The role of KCNQ1/KCNE1 $K^+$ channels in intestine and pancreas: Lessons from the KCNE1 knockout mouse. *Pflügers Arch* 443: 882–828, 2002.
63. **Warth R and Bleich M.** $K^+$ channels and colonic function. *Rev Physiol Biochem Pharmcol* 140: 1–62, 2000.
64. **Wegmann M, Kämpen A, Weber S, Seyberth HW, and Köckerling A.** Effect of hydroxyeicosatetraenoic acids on furosemide-sensitive $Cl^-$ secretion in rat distal colon. *J Pharmacol Exp Ther* 295: 133–138, 2000.
65. **Yang WP, Levesque PC, Little WA, Conder ML, Shalaby FY, and Blanar MA.** $K_V$LQT, a voltage-gated $K^+$ channel responsible for human cardiac arrhythmias. *Proc Natl Acad Sci USA* 94: 4017–4021, 1997.